

# PROPERTIES OF A STATISTICAL MODEL OF ICE AT LOW TEMPERATURES

G. T. BARKEMA<sup>‡</sup>

*Laboratory of Atomic and Solid State Physics*

*Cornell University*

*Ithaca, NY 14853-2501*

JAN DE BOER<sup>§</sup>

*Institute for Theoretical Physics, University of Utrecht*

*Princetonplein 5, P.O. Box 80.006*

*3508 TA Utrecht, the Netherlands*

## ABSTRACT

A simple statistical model for ice is presented, based on a point charge model for H<sub>2</sub>O. To simulate this model, a Monte Carlo algorithm is constructed that samples proton configurations according to the Boltzmann distribution. The ground state of the model is numerically found to be an ordered non-ferroelectric state with a unit cell of eight water molecules. The same structure has been previously proposed for the low-temperature phase of ice, called ice XI, on the basis of water-water potential calculations. The model is simulated at various temperatures, and the internal energy, entropy and static dielectric constant are obtained as a function of the temperature. The model has a phase transition towards the ground state at  $T = 36K$ , and no partial ordering is observed. This transition is compared with the phase transition towards ice XI in KOH-doped ice.

---

<sup>‡</sup>e-mail: barkema@helios.tn.cornell.edu

<sup>§</sup>e-mail: deboer@ruunts.fys.ruu.nl

# 1. Introduction

The statistical model for ice Ih (ordinary ice) introduced by Pauling [1] describes very accurately the observed residual entropy [2, 3] and is supported by nuclear magnetic resonance studies [4]. In this model, the oxygen atoms form a lattice with hexagonal symmetry (cf fig.1a ), and each oxygen atom has four neighbors such that the O–O bonds make approximately tetrahedral ( $\phi = \arccos(-1/3)$ ) angles with each other. The hydrogen atoms are distributed according to the Bernal-Fowler [5] rules or ice rules: each oxygen atom has precisely two hydrogen atoms attached to it at a distance  $\sim 1\text{\AA}$ , and precisely one hydrogen atom resides on each O–O bond. Actually, the protons reside on the O–O bonds, the electrons are not precisely localized, as they, together with the electrons from the oxygen atoms, form electron clouds that surround the water molecule. There are many ways to distribute the protons such that these rules are satisfied, and the assumption that these are all equally probable correctly predicts the residual entropy of ice mentioned before [6].

At temperatures far below the melting point, one expects that the interactions between the oxygen and hydrogen atoms become important and remove part of the disorder present in the Pauling model. This was first studied by Bjerrum [7] who used a point charge model to study the energy differences between different hydrogen configurations. Pitzer and Polissar [8] improved this calculation and suggested that ice undergoes a transition towards an ordered phase at a certain critical temperature  $T_c$ , and they estimated  $T_c$  to be about  $60K$ . Such a transition would significantly reduce the residual entropy. That this reduction of the residual entropy is not found in experiment is not in contradiction with the existence of a phase transition, because the protons ‘freeze in’ at about  $100K$  [3, 9], and below this temperature equilibrium is no longer reached in a reasonable time.

The fact that the protons are not frozen in above  $100K$ , and that the water molecules can reorient freely, is caused by the presence of two kinds of point defects in ice [7]: the Bjerrum D and L defects, and ionic defects. D and L defects correspond to the situation where either two or zero protons reside on an O–O bond, and ionic defects are those that violate the ice rule, so that an oxygen atom has

either one or three hydrogen atoms attached to it, which corresponds effectively to the presence of  $\text{OH}^-$  and  $\text{H}_3\text{O}^+$  ions respectively. These defects are thermally excited and can move around in the ice crystal by the correlative motion of protons on adjacent hydrogen bonds. They are also supposed to be responsible for many of the electrical properties of ice, as these can quite successfully be described in terms of defects [10, 11].

The proton mobility can be significantly enhanced by doping ice, which increases the number of defects. In ice doped with alkali hydroxides [12] equilibrium can still be reached at temperatures as low as  $60 - 65\text{K}$ . This is close to the estimated value  $T_c = 60\text{K}$  of Pitzer and Polissar for the transition towards an ordered phase, and suggests one might be able to observe this transition in doped ice. Evidence of its existence was first obtained in dielectric measurements on KOH-doped ice [13]. Subsequent calorimetric [14, 15] and dielectric [16, 17] measurements on KOH-doped ice showed that there is indeed a transition at  $72\text{K}$  towards an ordered phase, which is designated as ice XI [15], with a residual entropy that is 67% lower than the value for ordinary ice Ih. The same transition has also been observed in RbOH-doped ice [17], and in single crystals [18]. The structure of ice XI has been measured by neutron diffraction [19, 20]. These measurements show that in ice XI about 57% of the ice is ordered, forming domains that are less than about  $40\text{\AA}$  in dimension. Furthermore, they indicate that the ordered phase is ferroelectric, and that ice XI has a unit cell consisting of four water molecules with space group  $Cmc2_1$ . The same structure has been proposed by Kamb [21] and on the basis of a mean field calculation by Minagawa [22]. In these proposed structures it is assumed that ordered ice has a unit cell of four water molecules, and then only two ordered structure are possible [23]. If one assumes that the unit cell consists of eight molecules, there are 17 different conceivable ordered structures [23]. One of these, an non-ferroelectric structure with space group  $Pna2_1$ , was proposed for ice XI in [24], on the basis of the calculation of two- and three-body nearest neighbor water-water potentials.

In this paper we perform a Monte Carlo simulation of a point-charge model of ice, namely the

unit model introduced by Nagle [25], to find out whether such a model shares some of the features of real ice. The energies of different proton configurations were computed using a Coulomb potential, truncated at a certain distance. For a wide range of temperatures, we obtained the entropy, the internal energy (not taking into account the contributions due to vibrational and rotational degrees of freedom) and the static dielectric constant. This numerical approach to ice is new. Previous simulations did not take interactions into account besides the ice rules, and were thus restricted to infinite temperature. Estimates of energy differences between configurations have been made by hand, but only for the proton configurations around two neighboring oxygen atoms. In an appendix we summarize the method of Ferrenberg and Swendsen [26] which we used to compute these quantities from simulations at different temperatures. It turns out that our model has a phase transition towards the same non-ferroelectric ordered structure as proposed in [24]. We find no indications for any partial ordering.

## 2. The Unit Model

The point charge model of the water molecule we used in the simulations consists of an oxygen atom with charge  $-2q$ , and two hydrogen atoms with charge  $+q$  at a distance  $d_{OH}$  from the oxygen atom, under a relative angle  $\alpha$  (see fig 2). A water molecule in vapor has  $d_{OH} = 0.9572\text{\AA}$  and  $\alpha = 104.52^\circ$ . These values are for instance used in the TIP-4P model for the water molecule. In ice, these values are somewhat different. Older measurements give  $d_{OH} = 0.97\text{\AA}$  [21] up to  $d_{OH} = 1.01\text{\AA}$  [27]. More recent extensive neutron diffraction studies show that  $d_{OH} = 1.008(4)\text{\AA}$  for the position of the proton [28], but x-ray diffractometry, which takes also the positions of the electrons into account, yields values as low as  $0.85\text{\AA}$  [29]. In view of these latter measurements, we decided to take  $d_{OH} = 0.96\text{\AA}$ . For the angle  $\alpha$  we took the tetrahedral angle  $\alpha = 109.47^\circ$ , which is both convenient from the practical point of view and agrees perfectly well with experimental values for  $\alpha$  [28, 29]. The effective charge  $q$  of the

protons is difficult to measure directly; we fixed it by the requirement that the static dielectric constant of our model, determined by equation (4.2), agrees with the value  $\epsilon_s = 112$  measured by Gough and Davidson at  $T = 233K$  [30]. This yields  $q = 0.865e$ . This implies that the dipole moment of a water molecule with our parameters is  $10.7 \times 10^{-30} Cm$ , which is considerably larger than  $6.1 \times 10^{-30} Cm$ , the dipole moment of a water molecule in vapor. A direct measurement of the dipole moment of a water molecule in ice has not been achieved, but a calculation of Coulson and Eisenberg shows that it is certainly larger than the value in vapor [31].

The last parameter that enters in the model is the distance  $d_{OO}$  between two neighboring oxygen atoms. At temperatures around  $-40^\circ C$  it is  $2.76\text{\AA}$  [28, 29], and drops to approximately  $2.75\text{\AA}$  at  $-200^\circ C$  [32]. We took  $d_{OO} = 2.75\text{\AA}$ . This deviates less than 0.5 % from experimentally observed values for ice XI [19, 20].

From these parameters the effective charge of defects can be computed as  $e_B = 2qd_{OH}/d_{OO} = 0.60e$  [25] for the Bjerrum defects and  $e_I = e - e_B = 0.40e$  for the ionic defects. The values for  $e_B$  one encounters in the literature range from  $0.25e$  to  $0.55e$  (see [33]), so that our value for  $q$  seems somewhat large. However, because we sample from all possible proton configurations with a Boltzmann factor  $\exp(-H/k_B T)$ , where the hamiltonian  $H$  is given by the Coulomb energy

$$H = -\frac{1}{2\epsilon_\infty} \sum_{i \neq j} \frac{q_i q_j}{r_{ij}}, \quad (2.1)$$

and the sum is over all oxygen and hydrogen atoms, choosing a different value  $q' = \lambda q$  is equivalent to choosing a different temperature  $T' = T/\lambda^2$ . Thus, changing the value of  $q$  corresponds to scaling the temperature and has no effect on the qualitative behavior of our model. Notice that  $H$  in (2.1) is proportional to  $\epsilon_\infty = 3.1$ , the asymptotic value of the dielectric constant for increasing frequency. This factor accounts for the different ways in which the electron clouds are deformed as one varies the proton configuration.

The partition function of the model is given by

$$Z = \sum_{\substack{\text{proton} \\ \text{configurations}}} e^{-H/k_B T}, \quad (2.2)$$

where the sum is over all proton configurations that satisfy the Bernal-Fowler rules. In practice one has to restrict the calculation to a finite ice lattice, but one would in principle like to take the thermodynamic limit where the size of the lattice goes to infinity. Given an arbitrary proton configuration, one has the following upper bound for the energy of the configuration

$$E \leq \frac{1}{2\epsilon_\infty} \sum_{i \neq j} \frac{|q_i q_j|}{r_{ij}}, \quad (2.3)$$

but the latter sum grows as  $N^{5/3}$ , where  $N$  is the number of water molecules in the ice lattice, so that it is not clear that a proper thermodynamic limit exists. The unit model which we use was introduced by Nagle [25] and is not a new model for ice, but merely a way to rewrite (2.1) such that the energy of a proton configuration grows linearly with  $N$ . In the unit model, one assigns a cell  $C_a$  to each oxygen atom (labeled by  $a$ ) consisting of the oxygen atom, the two protons attached to it with a reduced charge  $q_{red}$ , and the two protons not attached to it with reduced charge  $q - q_{red}$ . Clearly, the union of all cells  $C_a$  is precisely the original configuration where all the hydrogen atoms have the proper charge, apart from charges at the surface of the finite ice lattice. The reduced charge  $q_{red}$  is determined by the requirement that  $C_a$  has no dipole moment, giving  $q_{red}d_{OH} - (q - q_{red})(d_{OO} - d_{OH}) = 0$ , so that

$$q_{red} = q \frac{d_{OO} - d_{OH}}{d_{OO}}. \quad (2.4)$$

At large distances,  $C_a$  can effectively be replaced by a quadrupole moment. Notice that the polarization of a finite ice lattice is now entirely due to the surface charge  $\mathcal{S}$ . Using the cells  $C_a$  the energy of a proton configuration can be rewritten as

$$E = -\frac{1}{2\epsilon_\infty} \sum_a \sum_{\substack{q_i, q_j \in C_a \\ i \neq j}} \frac{q_i q_j}{r_{ij}} - \frac{1}{2\epsilon_\infty} \sum_{a \neq b} \sum_{\substack{q_i \in C_a \\ q_j \in C_b}} \frac{q_i q_j}{r_{ij}} + E_{\text{surface}}, \quad (2.5)$$

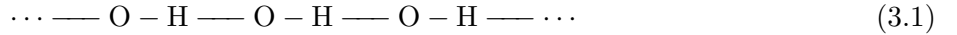
in which  $E_{\text{surface}}$  is the contribution from the surface charges. Because quadrupole-quadrupole interactions decrease as  $r^{-5}$ , the energy in (2.5) grows linearly with  $N$ . Naively,  $E_{\text{surface}}$  also grows linearly with  $N$ . To avoid having to take these contributions into account, we put an infinitely big metal container around our system. Due to this container, the contribution from the surface charges is suppressed and drops out in the limit where  $N \rightarrow \infty$ . In this case a finite ice lattice with periodic boundary conditions is a good description for the interior of a very large ice lattice, since periodic boundary conditions automatically exclude the presence of surface charges. The trick to divide the charges into ‘units’  $C_a$  guarantees a fast convergence of  $E$  for increasing distance between different units. If one does not do this, an accurate calculation of  $E$  may be quite difficult (cf. [8]).

### 3. The Algorithm

As explained before, we take a finite lattice with periodic boundary conditions and want to generate a sequence of proton configurations such that the probability that a particular configuration occurs is proportional to  $\exp(-E/k_B T_{\text{sim}})$ , where  $E$  is the energy of the configuration. The expectation value of a quantity at a temperature  $T_{\text{sim}}$  can then be found by simply taking the average of that quantity for the sequence of proton configurations. However, we can also obtain expectation values at temperatures  $T \neq T_{\text{sim}}$ , using a method published by Ferrenberg and Swendsen [26]. Our implementation of this method is outlined in the appendix.

To generate a sequence of proton configurations, some mechanism is required to change from one proton configuration to another. In real ice, the thermally generated defects are responsible for these changes. The mechanism that we used corresponds to the spontaneous arising of a pair of (either Bjerrum or ionic) defects and a recombination of this pair somewhere else in the lattice. The result of this process is equal to a change of proton positions on the bonds of a closed loop of O–O bonds in the oxygen lattice, in which all oxygen atoms that form the loop are attached to precisely one proton

on the loop. In other words, a piece of loop looks locally like



Already at  $-10^\circ\text{C}$  only about one in the five million sites is occupied by a Bjerrum defect, and the number of ionic defects is even less [34]. For a typical simulation on an ice lattice with 1000 sites, there will be no defects; furthermore in the presence of defects it is no longer possible to divide the proton configuration into units without the introduction of extra charges inside the lattice. Hence we did not incorporate actual defects.

We sampled proton configurations with a Metropolis-type algorithm [35], based on the dynamics described above. Given a configuration  $A$ , another configuration  $B$  is generated by changing the positions of the protons along a loop. A way to find such loops is to draw arrows along all the  $OHO$  bonds in the direction of the oxygen to which the proton is attached. Then one selects randomly a point in the ice lattice, and starts to walk around in the lattice, following the directions of the arrows; at each oxygen atom there are always two possibilities how to continue the walk, and one of these is picked with probability  $1/2$ . As the lattice is finite, this walk will self intersect at some site  $S$ . Part of the walk consists of a closed loop from  $S$  to  $S$ , and  $B$  is obtained from  $A$  by changing the positions of the protons along this loop. We denote the probability to propose a move from  $A$  to  $B$  by  $T_{AB}$ . As usual in Metropolis-type algorithms,  $B$  is accepted with a certain acceptance probability  $A_{AB}$ . If it is rejected, the next configuration is  $A$  rather than  $B$ . In this way one generates a sequence of configurations  $\{A_1, A_2, A_3, \dots\}$ . This sequence corresponds to a probability distribution  $P(A)$  of the configurations  $A$ . In equilibrium,  $P(A)$  should not change when applying one Metropolis step to it. Thus

$$0 \equiv \delta P(A) = - \sum_B P(A) T_{AB} A_{AB} + \sum_B P(B) T_{BA} A_{BA} \quad (3.2)$$

This equation is certainly satisfied and yields the Boltzmann distribution  $P(A) \sim \exp(-E(A)/k_B T)$



if for all  $A, B$

$$e^{-E(A)/k_B T} T_{AB} A_{AB} = e^{-E(B)/k_B T} T_{BA} A_{BA}, \quad (3.3)$$

which is known as the equation for detailed balance [36]. To proceed, we need to know something about  $T_{AB}$ .

Let  $L$  denote the loop that was used to generate  $B$  from  $A$ , and  $W_A(P, Q, l)$  denote the number of non self-intersecting walks on  $A$  from  $P$  to  $Q$  of length  $l$  that do not intersect  $L$ . Then  $T_{AB}$  can be written as

$$T_{AB} = \frac{1}{N} \sum_P \sum_{Q \in L} \sum_l 2^{-l-|L|} W_A(P, Q, l), \quad (3.4)$$

where  $|L|$  is the length of  $L$ . Because  $W_A(P, Q, l) = W_B(P, Q, l)$  it is clear from (3.4) that  $T_{AB} = T_{BA}$ .

Due to this observation, (3.3) reduces to

$$\frac{A_{AB}}{A_{BA}} = e^{(E(A)-E(B))/k_B T}, \quad (3.5)$$

and the best choice for  $A_{AB}$  is

$$A_{AB} = \min(1, e^{(E(A)-E(B))/k_B T}). \quad (3.6)$$

In the case where  $T \rightarrow \infty$  when all configurations are equally probable, this algorithm has been introduced for three-dimensional hexagonal and cubic ice by Rahman and Stillinger [37] and has been used for the computation of correlation functions for two-dimensional square ice by Yanagawa and Nagle [38], although it was not shown in these papers that the equilibrium distribution for  $A_{AB} = 1$  indeed corresponds to the infinite temperature Boltzmann distribution.

The ergodicity of this algorithm has been shown by Griffiths [39]. Actually, it is very easy to see that all configurations can be reached from one starting configuration and thus to prove ergodicity. As is illustrated in fig. 3 for two-dimensional square ice, the difference between two configurations can always be decomposed in a finite number of directed loops. Consecutively changing the proton

positions on these loops will generate one configuration from the other; of course the same argument is also valid for three-dimensional ice.

It is important that we allow loops that pass through the periodic boundary conditions. In the real system, that we placed inside a metal container, they correspond to loops passing through the metal. If we do not incorporate these loops, the total net polarization within one periodic cell (the sum of the dipole moments of the water molecules) would never change, and ergodicity would not be satisfied.

This completes the description of the model, we now turn to the results of the Monte Carlo simulations.

## 4. Results

The simulations were performed in parallel on two to four processors, each processor simulating its own lattice. Each lattice consisted of  $14 \times 10 \times 10$  water molecules; after reversing the deformation process as scheduled in fig 1, this corresponds to a roughly cubic system with dimensions  $31.44 \times 38.89 \times 36.67\text{\AA}$ . Larger lattices are unfeasible for computational reasons.

As illustrated in figures 1b and 1c, the ice lattice can be deformed into a lattice consisting of two dimensional ‘brick’ layers. The latter can easily be represented in a three-dimensional array, which makes storage of the proton configurations easy.

The energy of a proton configuration was computed using the unit model described in section 2. We used a cut-off radius for the quadrupole-quadrupole interactions of  $3d_{OO} = 8.25\text{\AA}$ , *i.e.* we ignored all interactions between all unit cells further than  $3d_{OO}$  apart. We estimate that the error due to this cut-off is  $\sim 2\%$ . If we took only nearest neighbor interactions into account, the errors were as large as 30%. In general, energy differences become smaller if the cut-off radius is enlarged. Thus, even if

we introduce unit cells to eliminate net charges and dipole moments, we still need to go beyond the nearest neighbor approximation in this model.

We started our simulations at  $T = 20K$  with a non-ferroelectric ordered state with a unit cell consisting of 8 water molecules with space group  $Pna2_1$ , as discussed in the introduction. The proton configuration is given by fig 4. Although we have no rigorous proof, there are strong indications that this is the ground state of our model. In all our simulations, we never encountered any configuration with a lower energy, and if we compare the energy of this configuration with the ferroelectric one proposed in [19, 20, 21, 22], we find a considerable energy difference of  $5.2K$  per molecule in favor of our starting configuration, into which the ferroelectric one decayed in the simulations at low temperatures.

Simulations were performed at 20,30,35,40,50,100,200,300,400,500,600K, in that order. Although the last four temperatures are physically irrelevant, because of the Ferrenberg-Swendsen algorithm (see appendix) the data obtained at these temperatures can be used to get more accurate estimates of quantities at low temperatures. For the initial configuration of the simulations at  $T > 20K$ , we took the end configuration of the previous temperature. For each temperature,  $2 \times 10^5$  steps were taken, of which the first  $5 \times 10^4$  were used for thermalization. Every 100 steps, the quantities  $E, f_c, f_h, G$  were stored, yielding a list of 1500 values for these four quantities at each temperature. The meaning of these quantities is as follows.

$E$  is the energy of the proton configuration, which we need to compute the internal energy and the entropy. To explain the meaning of the quantities  $f_c$  and  $f_h$ , consider an O–O bond in the  $c$ -direction. There are 18 possible ways to attach four protons to these two oxygen atoms in a way that satisfies the ice rule. If we restrict for a moment the Coulomb interactions to these two oxygen atoms and the four protons only, then there are essentially only two different configurations. The six configurations that are energetically more favorable are usually called inverse mirror configurations, the other twelve are the so-called oblique mirror configurations [7, 8]. In the same way the 18 configurations along an O–O bond in the  $h$ -direction can be divided into 12 energetically more favorable oblique center

configurations and six less favorable inverse center configurations. Now  $f_c$  is the percentage of bonds in the  $c$ -direction along which the configuration is oblique mirror, and  $f_h$  is the percentage of bonds in the  $h$ -direction along which the configuration is inverse center. At infinite temperature,  $f_c = 66.7\%$  and  $f_h = 33.3\%$ . As the temperature gets lower, one expects that both  $f_c$  and  $f_h$  tend to zero. For our ground state they are indeed zero. The reason that we took track of  $f_c$  and  $f_h$  separately, is to find out whether the ordering in the  $c$ -direction takes place at the same temperature as the ordering in the  $h$ -direction, or whether there are maybe two different phase transitions (which might account for the fact that only part of the residual entropy is lost in the phase transition to ice XI in KOH-doped ice). The last quantity  $G$  is related to the sum  $\vec{\Sigma}\mu$  of the dipole moments of the water molecules,

$$G = \frac{\vec{\Sigma}\mu \cdot \vec{\Sigma}\mu}{N\mu^2}, \quad (4.1)$$

where  $\mu$  is the magnitude of the dipole moment of one water molecule. For the unit model, the Onsager-Slater theory [40] of the dielectric constant is exact [25], and gives the following relation between the static dielectric constant  $\epsilon_s$  and  $G$

$$\epsilon_s - \epsilon_\infty = \frac{4\pi N}{V} \frac{G\mu^2}{3k_B T}. \quad (4.2)$$

The results for the internal energy per molecule  $u$ , the entropy per molecule  $s$ , the percentages  $f_c$  and  $f_h$ , the polarization factor  $G$  and the static dielectric constant  $\epsilon_s$  are given in figures 5 to 9. We now discuss each of these in turn.

The internal energy in figure 5 has a very sharp transition at  $T = 36.6K$ , where the specific heat  $c_v = \partial u / \partial T$  takes its maximum value of 10. Note that if we express the internal energy in Kelvin, the specific heat is dimensionless. The maximum value of the specific heat strongly depends upon the lattice size. For a lattice consisting of  $10 \times 6 \times 6$  water molecules, we found  $c_v(\text{max}) = 1.1$ , and for a  $12 \times 8 \times 8$  lattice,  $c_v(\text{max}) = 2.0$ . This shows that the system has a phase transition. In real ice, the internal energy also gets contributions from vibrational and rotational degrees of freedom,

but these behave smoothly and will not affect the phase transition. To determine the order of the transition purely numerically is very difficult. Because the non-ferroelectric ground state in our model has many short closed loops along which one can displace the protons while still satisfying the ice rule, we expect on general grounds that the transition is of second order [14, 41]. In the proposed ferroelectric ground state configuration with a unit cell of four water molecules, such short loops do not exist, only loops that pass through the periodic boundary conditions, and if this were the ground state, the transition would probably be of first order. From calorimetric measurements on KOH-doped ice it was concluded in [14] that the transition at  $72K$  is of first order, which is additional evidence that ice XI has a ferroelectric ordered structure.

The entropy per molecule in fig. 6 shows a sharp transition similar to the one for the internal energy. At the transition, the entropy drops to zero, showing that ice is completely ordered below the transition temperature. The dashed line indicates the theoretically computed value of  $s = \log(1.50685) = 0.41$  for the entropy of ice at infinite temperature [6]. In our simulations, we obtained  $s = 0.422$  at infinite temperature.

Figure 7 shows  $f_c$  (upper curve) and  $f_h$  (lower curve). The dashed lines are the theoretical values at infinite temperature. The important thing that can be seen from this figure is that there is only one phase transition, the ordering occurs simultaneously along both the  $c$ - and  $h$ -bonds. This happens despite the fact that the energy difference (not taking the rest of the configuration into account) between oblique and center symmetric unit cells is more than twice as large as the difference between oblique and center mirror unit cells. Thus, we find no indication of any partial ordering in our model.

The polarization factor in figure 8 shows the behavior reminiscent of a transition towards a non-ferroelectric phase. If the transition were towards a ferroelectric phase,  $G$  would become very large at the critical temperature. The main difference between the behavior of  $G$  and that of the internal energy and the entropy is that below the transition temperature,  $G$  drops to zero very quickly, and that above the transition temperature  $G$  approaches much slower than  $u$  and  $s$  the infinite temperature

limit  $G(\infty) = 3.007(2)$ . This value agrees excellently with the theoretical value  $G(\infty) = 3.005$  [42], which is again indicated by a dashed line. Even at temperatures as high as  $273K$ ,  $G$  has only reached 85% of its final value.

The relevance of the factor  $G$  is that it is directly related to the static dielectric constant  $\epsilon_s$  in fig. 9 via (4.2). The squares in fig. 9 are the measured values taken from [30]. As we explained in section 2, we used the value of  $\epsilon_s$  at  $T = -40^\circ C$  to fix the value of the proton charge  $q$  in the unit model. The main reason why our value of  $q$  is quite large is because  $G$  is 2.44 instead of 3.00 at  $-40^\circ C$ . Most authors take  $G = 3$  if they compute  $q$  from  $\epsilon_s$ , and our simulations show that they may make a considerable error in doing so. There is an interesting qualitative difference between our values for  $\epsilon_s$  and the measured ones. In our case  $G \sim (\epsilon_s - \epsilon_\infty)T$  decreases with decreasing temperature. The measured values for  $\epsilon_s$  correspond, however, to an increasing  $G$ . If one assumes a Curie-Weiss like behavior for  $\epsilon_s$ , one finds that  $G$  is proportional to  $(1 - T_c/T)^{-1}$ , where  $T_c$  is the Curie-Weiss temperature. Our simulations correspond to negative  $T_c$ , but a fit of this behavior of  $G$  with the measured data gives  $T_c = 38K$  [43],  $T_c = 32K$  [30],  $T_c = 43K$  [45], and  $T_c = 15K$  [44]. However, in our opinion this behavior of  $G$  is not related to some Curie-Weiss like transition, but should rather be attributed to the behavior of the defects in ice. More sophisticated theories of the dielectric constant [10, 11] show that  $G$  depends on the densities and mobilities of the number of Bjerrum and ionic defects, and an explanation of the increase of  $G$  can be given purely in terms of these defects. Near the phase transition, the qualitative behavior of  $\epsilon_s$  looks quite similar to that in KOH-doped ice [16].

If one is interested in investigating the anisotropy of the static dielectric constant, one has to keep track of the polarization tensor  $G_{ij}$ , which is a direct generalization of (4.1)

$$G_{ij} = \frac{(\vec{e}_i \cdot \vec{\Sigma}\mu)(\vec{e}_j \cdot \vec{\Sigma}\mu)}{N\mu^2}, \quad (4.3)$$

where  $\vec{e}_i$  are unit vectors. We also computed  $G_{ij}$ , and found a very small anisotropy  $(2G_{zz} - G_{xx} - G_{yy})/G \sim 0.01$ . This means that the anisotropy in  $\epsilon_s$  is not larger than 1%, which is in agreement

with [44], although in older experiments anisotropies up to 12% were found [46]. An estimate for  $G$  based on a series expansion also shows a negligible anisotropy [47]. On the other hand, in [11] the possibility is discussed that the anisotropy in the dielectric constant is caused by an anisotropy in the Bjerrum charge rather than in  $G$ . If this is indeed the case, then the anisotropy cannot be predicted by our model.

Above the critical temperature, the statistical errors for  $u, s$  are  $\sim 0.1\%$ , for  $f_c, f_h \sim 1\%$  and for  $G$  approximately  $0.5\%$ . If the lattice is not too small, the correlation time at high temperatures can be shown to be equal to  $\tau = N/2\bar{l}$ , where  $\bar{l}$  is the average length of the loops along which the proton configurations are changed every step. For simulations on a  $14 \times 10 \times 10$  lattice, with a typical value  $\bar{l} = 10$ , we find  $\tau = 70$  steps, so that these correlations are effectively eliminated by taking a data point only every 100 steps, and certainly no significant correlation exist at the time scale of one complete run. Below the critical temperature however, the correlation functions has a long tail as the system tends to get stuck in a particular low energy state. These long tails introduce extra errors in the results that affect especially the entropy. We measured a difference between the entropy at zero and at infinite temperature of  $s(\infty) = 0.422$ , whereas the theoretical value is  $s(\infty) = 0.41$ . This shows that the systematic error is of the order of  $3\%$  at low temperatures. The measurements of  $u(\infty)$  and  $G(\infty)$  are hardly influenced by the systematic errors, and are much more accurate.

## 5. Conclusions

A phase transition of ice Ih, in which proton configurations are constrained only by the ice rules, towards ice XI, which has an ordered proton configuration, is observed by doping ice with alkali hydroxides [14, 15, 16, 17]. This phase transition is generally believed to be caused by energy differences between these proton configurations. Our model samples these proton configurations at several temperatures and for the first time energy differences are calculated beyond nearest neighbor interactions.

We found a non-ferroelectric ground state and a phase transition towards it at  $T = 36K$ . In real ice, the transition is at  $72K$  towards a partially ordered phase, and experiments [19, 20] indicate that the structure of this phase, ice XI, consists of small ordered polar domains embedded in a disordered configuration.

The discrepancy between our results and experiments has two lines of explanations:

Real ice is a very difficult quantum mechanical system, and one may question whether it is allowed to make such gross simplifications as we did. Many aspects of ice were not taken into account in our model: we did not take into account that the charges in real ice are not localized, we ignored lattice vibrations and deformations, and we did not take defects into account. One of these features might be responsible for the observed discrepancy.

The second possibility is that the transition in doped ice is only possible because of the presence of the alkali hydroxides in ice. The impurities cause a locally strong electric field in the ice lattice, that favors a polar state. One unit charge is capable of lowering the energy of the water molecules in a properly ordered ferroelectric domain with  $5.2K$  per molecule within a range of over a hundred Angstrom. Thus, one unit charge can be responsible for the formation of an ordered domain consisting of several thousands of water molecules. In that case, the transition we find would correspond to another one at even lower temperature. Unfortunately, this possibility cannot be checked by experiment, because even in doped ice the protons freeze in at about  $65K$ . To check this by means of computer simulations, we should simulate ice lattices with impurities, to see whether this changes the critical behavior. The formation of ordered domains is something that is at this moment beyond our computational abilities, as the size of these domains are comparable to the size of the largest lattices we can deal with.

As the energy difference between the ferroelectric configuration proposed for the ground state and the non-ferroelectric ground state of our model is quite large ( $5.2 K$  per molecule), the second line of explanation is much more likely, at least according to our opinion.



## Acknowledgements

We thank the ACCU center in Utrecht for ample computation time. This work was financially supported by the stichting voor Fundamenteel Onderzoek der Materie (FOM), and by the National Science Foundation under Contract No. DMR-91-21654 through the Materials Science Center and the Cornell National Supercomputer Facility.

## A. Appendix

In this appendix we briefly describe the method of Ferrenberg and Swendsen to use data obtained at different temperatures as optimally as possible [26].

Suppose that we perform a number of simulations of some system at inverse temperatures  $\beta_i = 1/k_B T_i, i = 1 \dots M$ . At each temperature  $T_i$  the simulation results in a sequence of states  $\psi_{i,k}, k = 1 \dots N_i$ , which we assume to be uncorrelated. It is straightforward to generalize the computation to the case where the sequence of states has a known correlation length  $\tau_i$  at each temperature. From the sequence of states  $\psi_{i,k}$  we want to estimate the density of states  $\rho(\psi)$  of the system. Because we a priori only know of the existence of the states  $\psi_{i,k}$ , the only reasonable guess for  $\rho(\psi)$  is

$$\rho(\psi) = \sum_{i,k} a_{i,k} \delta(\psi - \psi_{i,k}), \quad (\text{A.1})$$

and the total number of states, which is usually unknown, is related to the  $a_{i,k}$  via  $N_{tot} = \sum a_{i,k}$ . Given a state density (A.1), the probability of finding in a simulation precisely the sequence  $\psi_{i,k}$ , is given by

$$P = \prod_{i,k} \left( \frac{a_{i,k} e^{-\beta_i E_{i,k}}}{Z_i} \right), \quad (\text{A.2})$$

where  $E_{i,k}$  is the energy of the state  $\psi_{i,k}$  and  $Z_k$  is defined by

$$Z_i = \sum_{q,r} a_{q,r} e^{-\beta_i E_{q,r}}. \quad (\text{A.3})$$

A choice for the  $a_{i,k}$  is obtained by maximizing the probability (A.2). This procedure for estimating parameters is known in statistics as the maximum likelihood procedure. Differentiating  $P$  with respect to  $a_{j,l}$  gives

$$\frac{1}{a_{j,l}} = \sum_i \left( \frac{N_i e^{-\beta_i E_{j,l}}}{Z_i} \right), \quad (\text{A.4})$$

so that the problem of finding  $a_{i,k}$  is reduced to the determination of  $Z_i$ . Substituting (A.4) in (A.3) we find

$$Z_i = \sum_{q,r} \frac{e^{-\beta_i E_{q,r}}}{\sum_s \left( \frac{N_s e^{-\beta_s E_{q,r}}}{Z_s} \right)}. \quad (\text{A.5})$$

This equation can be applied recursively to some set of initial values for  $Z_i$ . As the  $Z_i$  are only determined up to an overall factor, one can for instance take  $\sum_i Z_i = 1$  as normalization condition, which guarantees convergence of the equations (A.5). For the initial values one can for example take the 'naive' guess  $Z_i = \sum_{q,r} \exp((\beta_r - \beta_i) E_{rs})$ . An efficient implementation of this algorithm is obtained if, instead of using (A.5) with the sum over all  $r = 1, \dots, N_q$ , one first iterates (A.5) summing only over those  $r$  that are multiples of  $2^\alpha$  for some  $\alpha > 0$ , and then uses the resulting values for  $Z_i$  as initial values for the next set of iterations where  $r$  is restricted to multiples of  $2^{\alpha-1}$  etc.

After one has obtained the  $Z_i$ , one can fix the normalization by requiring  $\sum a_{q,r} = N_{tot}$ . If  $N_{tot}$  is unknown, one can take some arbitrary value for it. Most quantities are independent of  $N_{tot}$ , only the entropy is shifted by a constant if  $N_{tot}$  is changed. For a finite ice lattice, we know that  $N_{tot}$  is approximately  $(3/2)^N$ , and used this to fix the normalization. From the simulations one thus obtains the following estimate for the value of some quantity  $A$  as function of the temperature

$$A(\beta) = \frac{\sum_{q,r} a_{q,r} A(\psi_{q,r}) e^{-\beta E_{q,r}}}{\sum_{q,r} a_{q,r} e^{-\beta E_{q,r}}}. \quad (\text{A.6})$$

To do the computation, one needs a list  $\{\beta_q, A_l(\psi_{q,r}), E_{q,r}\}$ , where  $A_l$  are the quantities to be determined. The entropy is

$$S(\beta) = -k_B \beta^2 \frac{\partial}{\partial \beta} \left( \beta^{-1} \log \left( \sum_{q,r} a_{q,r} e^{-\beta E_{q,r}} \right) \right). \quad (\text{A.7})$$

To estimate the purely statistical errors in the quantities computed with this procedure, we use the following approximation.

First, consider a system with some discrete set of states, and let  $\psi_0$  denote a particular state, and  $Z(\beta)$  the partition function at inverse temperature  $\beta$ . If one extracts  $N$  independent states from the system while it is in equilibrium at inverse temperature  $\beta$ , the number  $N_0$  of states  $\psi_0$  in this sequence will satisfy a binomial distribution, and therefore the error in  $N_0$  is given by

$$\langle (\Delta N_0)^2 \rangle = Np(1-p) = \langle N_0 \rangle (1-p) \approx \langle N_0 \rangle, \quad (\text{A.8})$$

where  $p = \exp(-\beta E(\psi_0))/Z(\beta)$  is assumed to be small. Because one of the delta functions in the definition of  $\rho(\psi)$  (A.1) corresponds effectively to the occurrence of precisely one state, it follows that  $(\Delta \delta(\psi - \psi_{i,k}))^2 = \delta(\psi - \psi_{i,k})$ . The only way in which these errors occur in  $a_{i,k}$  is via  $Z_i$ , and if a reasonable number of states have been obtained at each temperature, *i.e.*  $N_i$  is not too small, then we can neglect the errors in  $Z_i$  and  $a_{i,k}$ . It is now easy to give a formula for the error in a quantity  $Q(\rho)$  that depends on the density of states  $\rho$ :

$$(\Delta Q)^2 = \int d\psi \left( \frac{\delta Q}{\delta \rho(\psi)} \right)^2 (\Delta \rho(\psi))^2, \quad (\text{A.9})$$

where

$$(\Delta \rho(\psi))^2 = \sum_{i,k} a_{i,k}^2 \delta(\psi - \psi_{i,k}). \quad (\text{A.10})$$

To apply this for instance to (A.6) we should read (A.6) as

$$A(\beta) = \frac{\int d\psi \rho(\psi) A(\psi) e^{-\beta E(\psi)}}{\int d\psi \rho(\psi) e^{-\beta E(\psi)}}. \quad (\text{A.11})$$

Using (A.9), one can see at which temperatures one should perform extra simulations in order to reduce the error as optimally as possible. One should keep in mind that if the real density of states does not behave very smoothly, the errors computed here can be much smaller than the real errors. A similar situation happens in the case when one performs a simple numerical integration of functions whose derivatives are large.

## Figure Captions

Fig. 1a: The oxygen lattice of ice Ih.

Fig. 1b: The oxygen lattice deformed such that the oxygen atoms lie in planes perpendicular to the  $h$ -axis.

Fig. 1c: The lattice deformed even further such that the oxygen atoms now form two-dimensional ‘brick’ layers.

Fig. 2: A point charge model for the water molecule. The values of the parameters are  $d=0.96\text{\AA}$ ,  $\alpha = 109.47^\circ$ , and  $q = 0.865e$ .

Fig. 3: An illustration of the ergodicity of the algorithm in two dimensions. The difference between two proton configurations (white dots and black dots) can be decomposed in a number of ordered loops, *i.e.* loops that pass through white and black dots alternately. The configurations satisfy periodic boundary conditions.

Fig. 4: The non-ferroelectric ground state configuration. The two kinds of layers, corresponding to planes perpendicular to the  $h$ -axis, show that the unit cell of this configuration contains eight oxygen atoms.

Fig. 5: The internal energy per molecule as a function of temperature.

Fig. 6: The entropy per molecule as a function of temperature.

Fig. 7: Percentage of bonds in the  $c$ -direction along which configurations are oblique mirror ( $f_c$ ), and of bonds along which configurations are inverse center ( $f_h$ ). Ordering appears to occur simultaneously for both kinds of bonds.

Fig. 8: The polarization factor  $G$  versus temperature.

Fig. 9: The static dielectric constant versus temperature. The squares are the measured values taken from [30].

## References

- [1] L. Pauling, J. Am. Chem. Soc. **57** (1935) 2680
- [2] W. F. Giaque and M. F. Ashley, Phys. Rev **43** (1933) 81
- [3] W. F. Giaque and J. W. Stout, J. Am. Chem. Soc. **58** (1936) 1144;
- [4] K. Kume, J. Phys. Soc. Japan **15** (1960) 1493; K. Kume and R. Hoshino, J. Phys. Soc. Japan **16** (1961) 290; N. N. Korst, V. A. Savel'ev and N. D. Sokolov, Sov. Phys. Sol. St. **6** (1964) 965; D. E. Barnaal and I. J. Lowe, J. Chem. Phys. **46** (1967) 4800; S. W. Rabideau and A. B. Denison, J. Chem. Phys. **49** (1968) 4660; G. Siegle and M. Weithase, in 'Physics of Ice', pp 571, Eds. N. Riehl, B. Bullemer and H. Engelhardt, Plenum Press, New York (1969)
- [5] J. D. Bernal and R. H. Fowler, J. Chem. Phys. **1** (1933) 515
- [6] J. F. Nagle, J. Math. Phys. **7** (1966) 1484
- [7] N. Bjerrum, K. Danske Vidensk. Selsk. Skr. **27** (1951) 1; Science **115** (1952) 385
- [8] K. S. Pitzer and J. Polissar, J. Chem. Phys. **60** (1956) 1140
- [9] S. Kawada, J. Phys. Soc. Japan **44** (1978) 1881; O. Haida, T. Matsuo, H. Suga and S. Seki, J. Chem. Thermodyn. **6** (1974) 815; O. Haida, H. Suga and S. Seki, J. Glaciology **22** (1979) 155
- [10] H. Gränicher, Z. Kristallogr. **110** (1958) 432; C. Jaccard, Helv. Phys. Acta **32** (1959) 89; A. Steinemann, Helv. Phys. Acta **30** (1957) 581; M. Hubmann, Z. Physik **B32** (1979) 141
- [11] C. Jaccard, Phys. Kondens. Materie **3** (1964) 99; M. Hubmann, Z. Physik **B32** (1979) 127
- [12] M. Ida, N. Nakatani, K. Imai and S. Kawada, Sci. Rep. Kanazawa Univ. **11** (1966) 13; M. Ida and S. Kawada, J. Phys. Soc. Japan **21** (1966) 561
- [13] S. Kawada, J. Phys. Soc. Japan **32** (1972) 1442

- [14] Y. Tajima, T. Matsuo and H. Suga, *Nature* **299** (1982) 810; *J. Phys. Chem. Solids* **45** (1984) 1135; T. Matsuo and H. Suga, *J. Phys. Paris* **48** (1987) C1-477; O. Yamamuro, M. Oguni, T. Matsuo and H. Suga, *J. Chem. Phys.* **86** (1987) 5137
- [15] T. Matsuo, Y. Tajima and H. Suga, *J. Phys. Chem. Solids* **47** (1986) 165
- [16] S. Kawada and H. Dohata, *J. Phys. Soc. Japan* **54** (1985) 477; S. Kawada, *J. Phys. Chem. Solids* **50** (1989) 1177
- [17] S. Kawada and K. Shimura, *J. Phys. Soc. Japan* **55** (1986) 4485
- [18] S. Kawada, I. Takei and H. Abe, *J. Phys. Soc. Japan* **58** (1989) 54
- [19] A. J. Leadbetter, R. C. Ward, J. W. Clark, P. A. tucker, T. Matsuo and H. Suga, *J. Chem. Phys* **82** (1985) 424
- [20] R. Howe and R. W. Whitworth, *J. Chem. Phys.* **90** (1989) 4450
- [21] B. Kamb, in 'Physics and Chemistry of Ice', pp. 28, Eds. E. Whalley, S. J. Jones and L. W. Gold, Royal Society of Canada, Ottawa (1973)
- [22] I. Minagawa, *J. Phys. Soc. Japan* **50** (1981) 3669; *J. Phys. Soc. Japan* **59** (1990) 1676
- [23] R. Howe, *J. Phys. (Paris) Colloq.* **48** (1987) C1-599
- [24] E. R. Davidson and K. Morokuma, *J. Chem. Phys.* **81** (1984) 3741; B. J. Yoon, K. Morokuma and E. R. Davidson, *J. Chem. Phys.* **83** (1985) 1223
- [25] J. F. Nagle, *Chem. Phys.* **43** (1979) 317
- [26] A. M. Ferrenberg and R. H. Swendsen, *Phys. Rev. Lett.* **61** (1988) 2635; **63** (1989) 1195
- [27] J. S. Chamberlain, F. H. Moore and N. H. Fletcher, in 'Physics and Chemistry of Ice', pp. 283, Eds. E. Whalley, S. J. Jones and L. W. Gold, Royal Society of Canada, Ottawa (1973)



- [28] W. F. Kuhs and M. S. Lehmann, *Nature* **294** (1981) 432; *J. Phys. Chem.* **87** (1983) 4312
- [29] A. Goto, T. Hondoh and S. Mae, *J. Chem. Phys.* **93** (1990) 1412
- [30] S. R. Gough and D. W. Davidson, *J. Chem. Phys.* **52** (1970) 5442;
- [31] C. A. Coulson and D. Eisenberg, *Proc. R. Soc.* **A291** (1966) 445
- [32] S. J. La Placa and B. Post, *Acta Crystallogr.* **13** (1960) 503; R. Brill and A. Tippe, *Acta Crystallogr.* **23** (1967) 343
- [33] I. Takei and N. Maeno, *J. Phys. (Paris) Colloq.* **48** (1987) 121
- [34] P. V. Hobbs, 'Ice Physics', Clarendon Press, Oxford (1974)
- [35] N. Metropolis, A. W. Rosenbluth, M. N. Rosenbluth, A. H. Teller and E. Teller, *J. Chem. Phys.* **21** (1953) 1087
- [36] D. Ceperley, G. V. Chester and M. H. Kalos, *Phys. Rev* **B16** (1977) 3081
- [37] A. Rahman and F. H. Stillinger, *J. Chem. Phys.* **57** (1972) 4009
- [38] A. Yanagawa and J. F. Nagle, *Chem. Phys.* **43** (1979) 329
- [39] A. Yanagawa, Ph.D. Dissertation, Carnegie-Mellon University, USA (1979)
- [40] L. Onsager and M. Dupuis, 'The Dielectrical Properties of Ice', *Rendiconti della Scuola Internazionale di Fisica 'E. Fermi', Corso* **10** (1960) 294; L. Onsager and M. Dupuis, in 'Electrolytes, The Electrical Properties of Ice', pp. 27, Ed. B. Pesce, Pergamon Press, New York (1962); L. Onsager and L. K. Runnels, *J. Chem. Phys.* **50** (1969) 1089; J. C. Slater, *J. Chem. Phys.* **9** (1941) 16
- [41] T. Matsuo, Y. Kume, H. Suga and S. Seki, *J. Phys. Chem. Solids* **37** (1976) 499
- [42] J. F. Nagle, in in 'Physics and Chemistry of Ice', Eds. E. Whalley, S. J. Jones and L. W. Gold, Royal Society of Canada, Ottawa (1973)

- [43] O. Wörz and R. H. Cole, *J. Chem. Phys.* **51** (1969) 1546
- [44] G. P. Johari and S. J. Jones, *J. Glaciology* **21** (1978) 259
- [45] Y. Sakabe, M. Ida and S. Kawada, *J. Phys. Soc. Japan* **28** (1970) 265
- [46] F. Humbel, F. Jona and P. Scherrer, *Helv. Phys. Acta* **26** (1953) 17; A. von Hippel, R. Mykolewycz, A. H. Runck and W. B. Westphal, *Tech. Rep. 10*, L.I.R., M.I.T., 1971
- [47] J. F. Nagle, *J. Chem. Phys.* **61** (1974) 883